#30

Papers from the GEOPHYSICAL LABORATORY
Carnegie Institution of Washington
No. 1745

American Mineralogist, Volume 63, pages 885–892, 1978

Predicted and observed compositional limits of trioctahedral micas

ROBERT M. HAZEN

Geophysical Laboratory
Carnegie Institution of Washington
Washington, D.C. 20008

AND DAVID R. WONES

Department of Geological Sciences
Virginia Polytechnic Institute and State University
Blacksburg, Virginia 24061

Abstract

A simple geometrical model of the stability limits of micas is based on the relative dimensions of octahedral and tetrahedral layers. If the tetrahedral rotation angle, α, is assumed to be limited to $0° \leq \alpha \leq 12°$, then the ratio of mean octahedral to mean tetrahedral metal–oxygen bond distances, d_o/d_t, is limited to $1.235 \leq d_o/d_t \leq 1.275$. Empirical ionic radii, bond expansivity, and bond compressibility data are used to predict geometrical pressure–temperature limits for several end-member trioctahedral micas.

Dehydration temperature for the reactions $KCo_3AlSi_3O_{10}(OH)_2 \rightleftarrows CoO + Co_2SiO_4 + KAlSi_2O_6 + H_2O$, $Co(OH)_2 \rightleftarrows CoO + H_2O$, and $Ni(OH)_2 \rightleftarrows NiO + H_2O$ were determined at several pressures. Actual mica stabilities are qualitatively in agreement with the predicted trend; for micas of the form $KR^{2+}_3AlSi_3O_{10}(OH)_2$, stability increases in the sequence Mn^{2+}, Fe^{2+}, Co^{2+}, Mg^{2+}, and Ni^{2+}. The predictions of mica stability limits are also consistent with observed compositional trends in natural micas.

Dehydration temperatures for hydroxides, $R^{2+}(OH)_2$, display the same sequence as the R^{2+} trioctahedral micas, though breakdown to the anhydrous phase plus H_2O occurs at significantly lower temperatures for the hydroxides. The difference between mica and hydroxide dehydration temperatures is due in part to shorter, stronger R^{2+}–OH bonds in the micas.

Introduction

An important goal of mineralogy is the understanding of solid–solid and solid–liquid stability relationships in terms of mineral structure and bonding. Experimental studies on the phase equilibria of mineral systems have been a major focus of mineralogists and petrologists for the past several decades. Crystallographers, similarly, have amassed an extensive literature on mineral crystal structures under room conditions, as well as structural variations with changing temperature and pressure. There have, however, been few studies in which experimental petrology and crystallography have been combined to elucidate details of mineral stability relationships. The trioctahedral micas provide an example where such a synthesis is possible.

The geometrical simplicity of the trioctahedral mica structure has resulted in the prediction of structural details from unit-cell and cation-radius data alone (Donnay *et al.*, 1964a; McCauley and Newnham, 1971; Hazen and Wones, 1972; Appelo, 1978). The variation of cation radius with composition is well known (Shannon and Prewitt, 1970), and effects of temperature and pressure on interatomic distances have been proposed by Hazen and Prewitt (1977) and Hazen and Finger (1977), and confirmed for phlogopite at high temperature (Takeda and Morosin, 1975) and at high pressure (Hazen and Finger, 1978). It is possible, therefore, to predict structural variations of trioctahedral micas as a function of temperature, pressure, and composition.

There appear to exist geometrical limits to possible trioctahedral mica structures, owing to the relative

0003-004X/78/0910-0885$02.00

sizes of octahedral and tetrahedral layers (Hazen, 1977; Guidotti *et al.*, 1975). If such geometrical limits exist, then it should be possible to predict, for various temperatures and pressures, ranges of mica composition that will not occur in nature. The principal objectives of this study are

(1) to describe possible geometrical limits of mica structures;

(2) to predict stability limits for several mica compositions as a function of temperature and pressure;

(3) to determine experimentally the stability field of cobalt trioctahedral mica, $KCo_3AlSi_3O_{10}(OH)_2$;

(4) to compare predicted stability limits with experimentally determined stability fields and natural occurrences of micas; and

(5) to compare observed stability curves for trioctahedral micas, $KR^{2+}_3AlSi_3O_{10}(OH)_2$, and the related hydroxides, $R^{2+}(OH)_2$.

Geometrical constraints on the mica structure

The stability of trioctahedral micas is limited by the fit of adjacent octahedral and tetrahedral layers, as measured by the tetrahedral rotation angle, α (Hazen and Wones, 1972, Fig. 8). If it is assumed that atomic fractional coordinates $z_{O1} = z_{O2}$ and $z_{O3} = z_{OH}$, that tetrahedra are regular, and that unit-cell $b = \sqrt{3}\,a$, then

$$\cos\alpha = 3\sqrt{3}\,d_o \sin\psi / 4\sqrt{2}\,d_t \qquad (1)$$

where d_o is the mean octahedral M–O distance, d_t is the mean tetrahedral M–O distance, and ψ is the octahedral flattening angle, which is approximately $59\pm1°$ in trioctahedral micas (Donnay *et al.*, 1964a). It is not possible for α to be negative, and observations of Guidotti *et al.* (1975) suggest that rotation angles in excess of 12° are rare, and may be unstable for trioctahedral micas. If

$$\sin\psi \approx 1.154 - 0.144\,d_o \qquad (2)$$

(after Hazen and Wones, 1972, Fig. 7), then the limits on α ($0° \leq \alpha \leq 12°$) imply that the ratio of octahedral to tetrahedral M–O distances, d_o/d_t, is also limited to $1.235 \leq d_o/d_t \leq 1.275$[1]. Because the effects of T, P, and X on d_o/d_t are known, it is possible to predict the value of α and consequently ranges of probable mica geometrical instability.

A useful observation in predicting d_o/d_t is that, for a given tetrahedral-layer composition, d_t is approximately invariant with T or P. Each tetrahedral-layer composition, therefore, is characterized by critical maximum and minimum values of d_o, associated with values of $\alpha = 0°$ and 12°, respectively. The critical values of d_o for a given d_t may be attained through changes in pressure, temperature, or octahedral layer composition, because all these variables alter d_o without changing d_t.

Predictions of compositional limits of trioctahedral micas

Calculation of the upper temperature stability limits of trioctahedral micas ($\alpha = 0°$) has been presented by Hazen (1977). In summary, micas of the composition $KR^{2+}_3AlSi_3O_{10}(OH)_2$ have a mean tetrahedral cation–anion distance of 1.649A (Hazen and Burnham, 1973). The possible values of d_o for this d_t are, from equations (1) and (2) above, $2.035 \leq d_o \leq 2.110$A. At room temperature and pressure, d_o for pure phlogopite is ≈2.06A (Hazen and Burnham, 1973). For $^{VI}Mg^{2+}$–O bonds, mean thermal expansion is $\bar{\alpha} = 14 \times 10^{-6}\ C^{-1}$ and mean compression is $\bar{\beta} = 17 \times 10^{-5}\ kbar^{-1}$ (Hazen and Prewitt, 1977). Critical equations for the upper and lower geometrical stability of pure phlogopite are (P in kbar, T in °C)

$$2.060(1 - 0.00017P + 0.000014T) \cong 2.110, \text{ or}$$

$$T \cong 12P + 1700 \text{ (upper limit)}, \qquad (3)$$

and

$$2.060(1 - 0.00017P + 0.000014T) \cong 2.035, \text{ or}$$

$$T \cong 12P - 900 \text{ (lower limit)}. \qquad (4)$$

These P–T lines represent upper and lower geometrical limits to phlogopite stability, based on the geometrical assumptions outlined above. They *do not* represent the actual P–T stability of phlogopite, which melts significantly below temperatures of equation (3) (Yoder and Kushiro, 1969).

Critical P–T lines for other end-member micas of the form $KR^{2+}_3AlSi_3O_{10}(OH)_2$ may be derived in a similar way if the values of d_o are based on Shannon and Prewitt (1970) radii. Specifically, d_o for Ni, Co, Fe, and Mn are 2.030, 2.085, 2.120, and 2.170A, respectively. Values of $\bar{\alpha}$ and $\bar{\beta}$ from Hazen and Prewitt (1977) are used to obtain maximum and minimum equations for critical limits of end-member micas (P in kbar, T in °C):

[1] More rigorous formulae for predicting mica structural variations have been presented by McCauley and Newham (1971) and Appelo (1978). The parameters calculated from equations (1) and (2) are similar to those of the more complex formulations and are therefore sufficient for one to predict relative stabilities of trioctahedral micas with different compositions.

	upper limit ($\alpha = 0°$)	lower limits ($\alpha = 12°$)
Ni	$T = 11P + 2800$	$T = 11P + 200$
Co	$T = 12P + 900$	$T = 12P - 1700$
Fe	$T = 13P - 300$	$T = 13P - 2900$
Mn	$T = 14P - 2000$	$T = 14P - 4600$

Note that divalent iron and manganese end-member trioctahedral micas are not stable under room conditions because the octahedral layer is too large. Nickel mica, on the other hand, has critically small octahedra and is predicted to have a tetrahedral rotation angle slightly greater than 12° under room conditions.

Ideal trioctahedral micas [$KR^{2+}_3AlSi_3O_{10}(OH)_2$] with large divalent octahedral cations (Fe^{2+},Mn^{2+}) are geometrically unstable because d_o/d_t exceeds 1.275. Iron and manganese micas can be stabilized, however, by at least four common substitutional modifications:

(1) $^{IV}Al^{3+} + {}^{VI}Al^{3+} \rightleftarrows {}^{IV}Si^{4+} + {}^{VI}R^{2+}$ (aluminum substitution)

(2) $^{VI}R^{2+} + (OH)^- \rightleftarrows {}^{VI}R^{3+} + O^{2-}$ (oxidation)

(3) $^{IV}Al^{3+} \rightleftarrows {}^{IV}Fe^{3+}$ (tetrahedral ferric iron substitution)

(4) $2^{VI}R^{2+} \rightleftarrows Ti^{4+} + \square$ (titanium + vacancy substitution).

Each of these modifications causes a reduction in d_o/d_t and consequently an increase in fit between octahedral and tetrahedral layers of iron and manganese micas.

Consider mechanism (1) in detail. Micas of the form $K(R^{2+}_{2.50}Al_{0.50})(Al_{1.50}Si_{2.50})O_{10}(OH)_2$, for which $d_t \cong 1.67$A, have critical limits on d_o of $2.06 < d_o < 2.13$A. The addition of 1/6 Al to the octahedral layer decreases mean octahedral M–O distances to $d_o \cong$ 2.000, 2.030, 2.050, 2.080, and 2.130 for divalent Ni, Mg, Co, Fe, and Mn, respectively. If these values are used, critical upper and lower stability limits for several micas of this type are (P in kbar, T in °C):

	upper ($\alpha \cong 0°$)	lower ($\alpha \cong 12°$)
Ni	$T = 11P + 4500$	$T = 11P + 2100$
Mg	$T = 12P + 3400$	$T = 12P + 1000$
Co	$T = 12P + 2800$	$T = 12P + 300$
Fe	$T = 13P + 1700$	$T = 13P - 700$
Mn	$T = 14P$	$T = 14P - 2400$

Aluminous micas with ($Al_{1.5}Si_{2.5}$) tetrahedral layer composition have critical geometrical limits calculated to be approximately 2000°C higher than for ($AlSi_3$) layers, for a given octahedral R^{2+} cation. Biotites rich in Fe^{2+} and Mn^{2+} consequently will be stabilized by this aluminum substitution (*i.e.* toward siderophyllite). Nickel mica, on the other hand, will not be stabilized with excess aluminum because α will increase above 12°. A mica of composition $K(Ni_{2.5}Al_{0.5})(Al_{1.5}Si_{2.5})O_{10}(OH)_2$ is predicted to have a tetrahedral rotation of ≈18° under room conditions. Note that pure eastonite is also predicted to be unstable, owing to its low value of d_o/d_t.

Effects of octahedral cation oxidation are similarly dramatic. Pure annite [$KFe^{2+}_3AlSi_3O_{10}(OH)_2$] is predicted to be unstable; this ideal end member is not known in nature and has not been synthesized (Hewitt and Wones, 1975). "Annites" of the composition $K(Fe^{2+}_{2.7}Fe^{3+}_{0.3})(AlSi_3)O_{10.3}(OH)_{1.7}$ have been synthesized, however. The values of d_o and d_t for this mica are ≈2.105 and 1.65A, giving $d_o/d_t = 1.275$, which is just within the possible range. This "critical structure" mica is predicted to have $\alpha = 0°$.

Another mica near annite composition that has been synthesized successfully is ferriannite, $KFe^{2+}Fe^{3+}Si_3O_{10}(OH)_2$ (Wones, 1963). In this mica, predicted d_o and d_t are 2.120 and 1.675A, respectively; $d_o/d_t = 1.265$, which is also in the possible range. The predicted value of α is 8°, compared with the observed value of 6° given by Donnay *et al.* (1964b).

Determination of mica and hydroxide stability

Previous studies

Several references include data on the stability of trioctahedral micas of the form $KR^{2+}_3AlSi_3O_{10}(OH)_2$. Yoder and Kushiro (1969) determined the stability limits and incongruent melting behavior of phlogopite to 37.5 kbar. A dehydration curve for nickel mica was presented by Klingsberg and Roy (1957), who found that the stability of $KNi_3AlSi_3O_{10}(OH)_2$ was virtually identical with that of phlogopite. Attempts to synthesize the pure end-member $KMn_3AlSi_3O_{10}(OH)_2$ and $KFe^{2+}_3AlSi_3O_{10}(OH)_2$ have proved unsuccessful (Lindqvist, 1966; Hazen and Wones, 1972; Hewitt and Wones, 1975), and it is assumed that these micas are not stable under room conditions. Eugster and Wones (1962), however, did present stability relationships for synthetic annites with small, but significant, amounts of ferric iron in the octahedral sites. Cobalt trioctahedral mica has been synthesized by Lindqvist (1966) and Hazen and Wones

(1972), but stability data have not been previously recorded.

Several authors, including MacDonald (1955) and Barnes and Ernst (1963), have presented data on the brucite $\rightleftarrows$ periclase + water reaction. Pistorius (1962) determined dehydration temperatures for $Co(OH)_2$ and $Ni(OH)_2$ from 5 to 100 kbar. Equilibrium curves for $Fe(OH)_2$ and $Mn(OH)_2$ were not found in the literature. Bernal *et al.* (1959), however, reported that $Fe(OH)_2$ decomposes into $FeO + H_2O$ at approximately 200°C in an atmosphere of dry nitrogen. Furthermore, Eh–pH plots for manganese and iron (Garrels and Christ, 1965) suggest that $Mn(OH)_2$ and $Fe(OH)_2$ may have similar stability characteristics.

Experimental

Synthesis and reversed runs have been used to determine the stability of $Co(OH)_2$, $Ni(OH)_2$, and $KCo_3AlSi_3O_{10}(OH)_2$. Hydroxide–oxide experiments were performed using $Co(OH)_2$ and $Ni(OH)_2$ prepared by the Edison precipitation method (Hazen and Wones, 1972), and reagent-grade CoO and NiO as starting materials. Experiments at pressures from 0.2 to 2.0 kbar extend to low pressure the 5 to 100 kbar data of Pistorius (1962). Starting material for $KCo_3AlSi_3O_{10}(OH)_2$ dehydration experiments was a gel as described by Hazen and Wones (1972).

Temperatures were measured with sheathed, calibrated thermocouples at the beginning and end of experiments. Thermocouple assemblies were calibrated against the melting point of NaCl (801°C) in glass capsules mounted within the pressure vessel assembly. This procedure also results in estimates of thermal gradients. Pressures were measured on a factory-calibrated Heise gauge. Experiments performed at 10 kbar were done at the Geophysical Laboratory by G. E. Speicher using an internally-heated pressure vessel, and were calibrated separately from the other experiments (Yoder and Kushiro, 1969).

Results

Results of synthesis and reversed runs are listed in Table 1, and dehydration curves for trioctahedral micas are illustrated in Figure 1. Unit-cell data for synthetic micas and hydroxides are listed in Table 2. These data show that the order of mica stability from low to high temperature is Mn, Fe, Co, and Mg = Ni. It should be noted that Fe and Mg micas form olivine + leucite + kalsilite, whereas Co and Ni micas form olivine + leucite + R^{2+} oxide. The four mica dehydration curves, therefore, are not strictly analogous.

Hydroxide equilibria are illustrated in a $\log f(H_2O)$ *vs.* $1/T$ plot (Fig. 2) along with mica dehydration lines. Note that hydroxides have relative positions similar to those of the micas, but they are significantly lower in absolute stability. Low-pressure data for $Co(OH)_2$ and $Ni(OH)_2$ presented in this study are in close agreement with the high-pressure data of Pistorius (1962).

Discussion

Comparison of predictions with experimental stability fields

Predictions of the stability limits of micas of the form $KR_3^{2+}AlSi_3O_{10}(OH)_2$ suggest that the geometrical limits of Ni mica are at higher temperature than those of phlogopite, which are greater than those of Co mica. Ferrous iron mica, annite, is predicted to be unstable, but minor oxidation or substitution of Fe^{3+} for Al should produce a geometrically stable mica. Predictions also suggest that pure Mn mica is not geometrically stable.

These predictions are consistent with experimentally-determined mica stabilities. Nickel and magnesium micas have the highest stabilities, whereas Co mica has a somewhat lower stability field. Manganese and ferrous iron micas appear to be unstable, but a modified annite with minor Fe^{3+} has been produced (Eugster and Wones, 1962).

Comparison of predictions with natural mica compositions

It has been suggested that micas are geometrically stable for only a relatively small range of d_o/d_t, but that this ratio is easily achieved by small degrees of cation substitution or oxidation. Distribution of natural trioctahedral mica compositions supports this concept. In the phlogopite–annite series the tendency for iron- and manganese-rich micas to have excess R^{3+} has been well documented (Foster, 1960). Magnesium-rich micas, on the other hand, have a limited range of octahedral Al substitution (Hewitt and Wones, 1975). The most aluminous Mg-rich mica plotted by Foster (1960, Fig. 11) is of the approximate composition $K(Mg_{2.6}Al_{0.4})(Al_{1.4}Si_{2.6})O_{10}(OH)_2$. The calculated α for this composition is $\approx 14°$. It is possible, therefore, that this mica, as well as more aluminous Mg-micas, is metastable under room conditions.

Geometrical analysis of micas may also provide information on possible cation distributions between octahedral and tetrahedral layers. Frondel and Ito (1966), for example, described a new species of Zn–

Table 1. Experiments determining the position of univariant equilibria

T, °C	P, bars	t, hr	Starting material (% H_2O)	Products
			(a) $Co(OH)_2 = CoO + H_2O$	
208±3	228±10	45	$CoO + Co(OH)_2 + H_2O$	$Co(OH)_2 + H_2O$
216±5	200±5	20	$Co(OH)_2 + H_2O$	$CoO + H_2O$
240±3	2000±10	24	$CoO + Co(OH)_2 + H_2O$	$Co(OH)_2 + H_2O$
243±4	2000±10	24	$Co(OH)_2 + H_2O$	$Co(OH)_2 + CoO + H_2O$
243±4	2000±10	24	$CoO + H_2O$	$CoO + H_2O$
249±3	2000±10	96	$Co(OH)_2 + H_2O$	$CoO + H_2O$
			(b) $Ni(OH)_2 = NiO + H_2O$	
244±6	214±10	24	$Ni(OH)_2 + H_2O$	$Ni(OH)_2 + H_2O$
256±3	200±5	43	$Ni(OH)_2 + H_2O$	$Ni(OH)_2 + NiO + H_2O$
249±4	2000±10	96	$Ni(OH)_2 + H_2O$	$Ni(OH)_2 + H_2O$
273±3	2000±10	24	$Ni(OH)_2 + H_2O$	$Ni(OH)_2 + H_2O$
281±4	2000±20	67	$NiO + H_2O$	$NiO + H_2O$
			(c) $KCo_3AlSi_3O_{10}(OH)_2 = CoO + Co_2SiO_4 + KAlSi_2O_6 + H_2O$	
798±3	100±5	41	Gel	CoPh + CoO + CoOl + Lc + H_2O
812±5	100±5	27	Gel	CoO + CoOl + Lc + H_2O
820±5	103±5	69	CoO + CoOl + Lc + H_2O	CoPh + CoO + CoOl + Lc + H_2O
825±5	100±5	24	CoO + CoOl + Lc + H_2O	CoO + CoOl + Lc + H_2O
794±5	110±20	72	Gel	CoPh + CoO + CoOl + Lc + H_2O
828±3	207±10	61	Gel	CoPh + CoO + CoOl + Lc + H_2O
855±5	200±10	24	CoO + CoOl + Lc + H_2O	CoPh + CoO + CoOl + Lc + H_2O
868±8	200±10	20	Gel	CoO + CoOl + Lc + H_2O
876±4	300±3	97	CoPh + H_2O	CoO + CoOl + Lc + H_2O
890±5	397±10	24	Gel	CoPh + CoO + CoOl + Lc + H_2O
890±5	397±10	24	CoO + CoOl + Lc + H_2O	CoPh + CoO + CoOl + Lc + H_2O
900	10,000	8	Gel (11% H_2O)	CoPh(98%) + CoO + gl
900	10,000	8	CoPh + CoOl + gl (5%)	CoPh
1000	10,000	4	Gel (8%)	CoOl + Lc + CoPh
1000	10,000	4	CoPh (15%)	CoPh + CoOl + gl
1050	10,000	6	CoOl + gl (6%)	CoPh + CoOl + gl
1050	10,000	6	CoOl + gl (4%)	CoPh + CoOl + CoO + gl
1100	10,000	4	Gel (6%)	CoOl + gl
1100	10,000	4	CoPh (4%)	CoOl + gl + CoPh(2%)

Mn trioctahedral mica from Franklin, New Jersey, which they named hendricksite. The composition of the mica varies considerably, but an average structural formula of approximately

$$K(Zn_{1.4}Mn^{2+}_{1.0}Mg_{0.3}Fe^{2+}_{0.03}Fe^{3+}_{0.25}Ti^{4+}_{0.02})^{VI}$$
$$(Si_{2.667}Al_{1.333})^{IV}O_{10}(OH)_2$$

is suggested by data in their Table 2 for micas #1–6. Hazen and Wones (1972) noted that some Zn^{2+} might be in the tetrahedral site in hendricksites and other zinc micas. The possible geometrical range of octahedral metal–oxygen bond distance, d_o, for a tetrahedral-layer composition of $(Al_{1.333}Si_{2.667})$ is $2.05 \leq d_o \leq 2.125$A. The calculated d_o for the average hen-

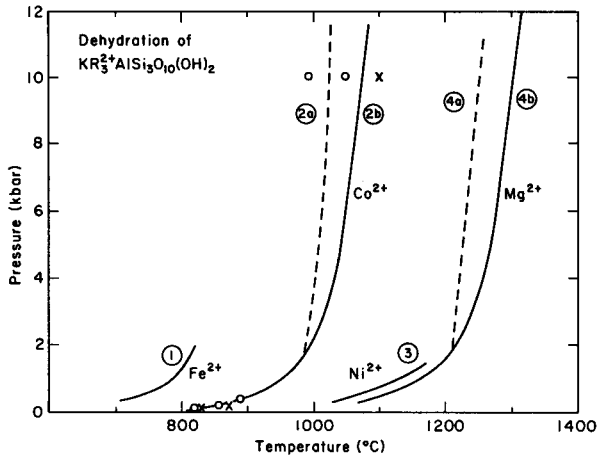

Fig. 1. Dehydration curves for micas of the type $KR_3^{2+}AlSi_3O_{10}(OH)_2$. (1) Annite ⇄ fayalite + leucite + kalsilite + H_2O (Eugster and Wones, 1962). (2a) $KCo_3AlSi_3O_{10}(OH)_2$ + H_2O ⇄ CoO + Co_2SiO_4 + melt. (2b) $KCo_3AlSi_3O_{10}(OH)_2$ ⇄ CoO + Co_2SiO_4 + $KAlSi_2O_6$ + H_2O (this study). (3) $KNi_3AlSi_3O_{10}(OH)_2$ ⇄ NiO + Ni_2SiO_4 + $KAlSi_2O_6$ + H_2O (Klingsberg and Roy, 1957). (4a) Phlogopite + H_2O ⇄ forsterite + kalsilite + melt. (4b) Phlogopite ⇄ forsterite + leucite + kalsilite + H_2O (Yoder and Kushiro, 1969).

dricksite, using radii of Shannon and Prewitt (1970), is 2.10A, which is well within the possible range ($\alpha \approx 5°$). It is not necessary, therefore, to have zinc in tetrahedral coordination for hendricksite to be stable.

Comparison of mica and hydroxide stabilities

At pressures below a few kilobars, stabilities of both micas and hydroxides are determined by dehydration reactions. For all octahedral cations studied, the upper temperature stability of the hydroxide is significantly lower than the mica stability (Fig. 2). The difference in free energy between water in equilibrium with hydroxide + oxide and water in equilibrium with mica + anhydrous assemblage may be determined directly from Figure 2 by measuring the vertical separation between the R^{2+} mica and hydroxide lines. For example, at 1000°K the brucite ⇄ periclase + H_2O line is 3.0 $\log_{10}f(H_2O)$ units above the phlogopite ⇄ olivine + leucite + kalsilite + H_2O line. Therefore,

$$\Delta G = RT \ln f_1/f_2 = 2.3RT(\log f_1 - \log f_2)$$
$$= 13.2 \text{ kcal/mole},$$

where f_1 and f_2 are the fugacity of water for brucite and phlogopite, respectively, at dehydration at 1000°C. This value is an approximate measure of the free energy of H_2O in equilibrium with mica, compared with hydroxide, at dehydration.

A difference in bonding between mica and hydroxide, which might be related to their differences in dehydration energy, is the length of the R^{2+}–OH bond. This distance is significantly longer in hydroxides than in micas, and the hydroxide R^{2+}–OH bond is, therefore, weaker than that in mica. For example, in brucite the Mg–OH distance is 2.10A (Elleman and Williams, 1956)[2], whereas the Mg–OH distance in phlogopite is 2.038A (Hazen and Burnham, 1973; McCauley *et al.*, 1973)[3]. This 3.0 percent difference in bond distance represents a similar difference in bond potential energy, U_{Mg-OH}. It is assumed that Mg–H interactions are the same for micas and hydroxides. For an isolated Mg–OH bond, potential energy from Coulombic attraction forces is

$$U_{Mg-OH} = \frac{q_1 q_2}{d_{M,OH}} = \frac{664.1}{d \text{ (in A)}} \text{ kcal/mole.}$$

[2] Elleman and Williams (1956) did not report the Mg–OH distance directly. They noted, however, that the oxygen atom is 1.04A above the plane of the magnesium atoms, which, combined with the unit-cell parameters, defines the Mg–OH distance.

[3] Mg–F in pure fluorophlogopite is 2.035A (McCauley *et al.*, 1973), and Mg–$(F_{0.7}OH_{0.3})$ is 2.036A (Hazen and Burnham, 1973). Mg–OH is therefore assumed to be approximately 2.038A.

Table 2. Unit-cell dimensions of synthetic hydroxides and micas

Compound	*a* (A)	*b* (A)	*c* (A)	β (°)	*V* (A^3)
$Ni(OH)_2$	3.125(1)*	...	4.628(2)	...	39.15(5)
$Co(OH)_2$	3.182(1)	...	4.653(2)	...	40.80(5)
$KMg_3AlSi_3O_{10}(OH)_2$	5.314(1)	9.206(2)	10.312(2)	99.90(3)	497.0(4)
$KNi_3AlSi_3O_{10}(OH)_2$	5.300(3)	9.173(1)	10.284(2)	99.88(3)	492.7(4)
$KCo_3AlSi_3O_{10}(OH)_2$	5.341(1)	9.240(1)	10.346(2)	99.93(3)	503.0(3)

**Parenthesized figures represent the estimated standard deviation (esd) in terms of least units cited for the value to their immediate left, thus 3.125(1) indicates an esd of 0.001.*

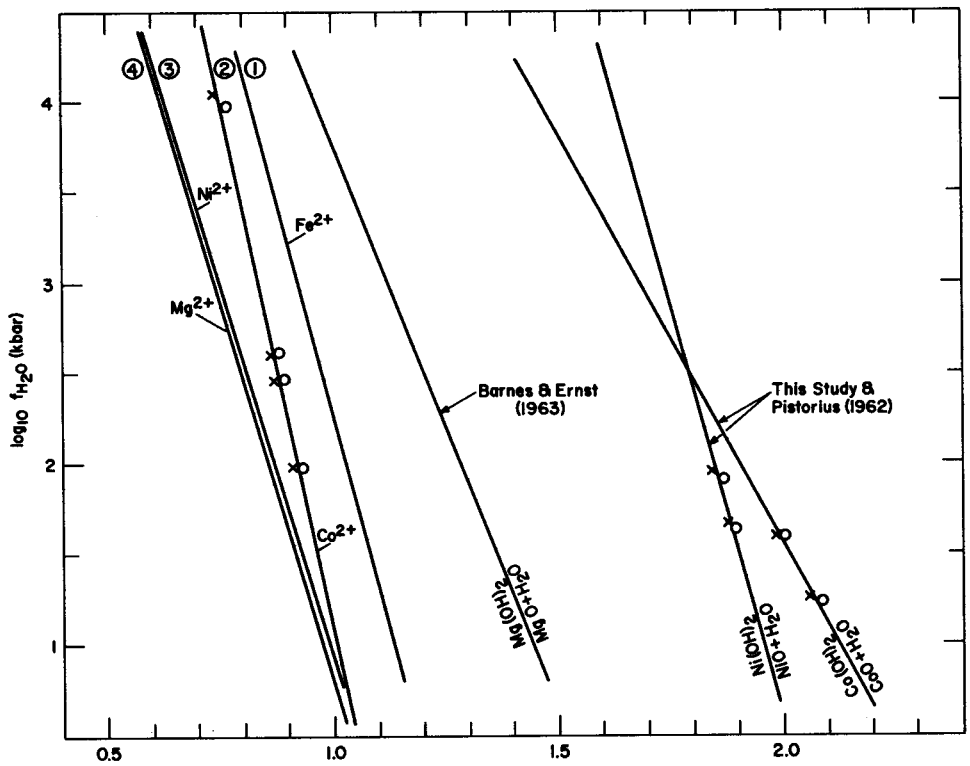

Fig. 2. Dehydration equilibria for micas and hydroxides. Points are calculated from P–T data using $\ln f(H_2O) = \ln f(P, T) - (\Delta V° P/RT)$. Values of $f(P, T)$ are from Burnham *et al.* (1969), and molar volumes of reactant and product phases are from Robie and Waldbaum (1968), Brown (1970), Hazen and Wones (1972), and the ASTM card file. Curves (1) to (4) are mica dehydrations, as listed in the caption of Fig. 1.

For isolated Mg–OH bonds of length 2.10 and 2.038A, the calculated bond potential energies are 316.3 and 325.9 kcal/mole, respectively. There are two Mg–OH bonds per formula unit of mica and hydroxide, so the difference in energy associated with Mg–OH bonds in brucite *vs.* phlogopite could be greater than 10 kcal/mole.

A fundamental goal of mineralogists is the determination of quantitative relationships between crystal structures and thermodynamic properties (see *e.g.* Slaughter, 1966). These relationships might ultimately lead to an understanding of the origins of phase transformations in terms of interatomic forces. A complete description of a phase transformation requires knowledge of the bonding and properties of all reactant and product phases. It is intuitively pleasing, however, to attach special significance to metal–hydroxide bonds in dehydration reactions. Any calculation of the potential energy associated with a bond within a structure requires consideration of the entire structure. Calculations of the potential energy of an isolated Mg–OH bond, for example, may not bear a direct relationship to the energy associated with Mg–OH bonds in phlogopite and brucite. It is nevertheless intriguing that the difference in potential energy between the shorter phlogopite Mg–OH bonds and the longer hydroxide Mg–OH bonds is calculated to be of the same order of magnitude as the difference in free energy of water associated with their dehydration. It is concluded that the higher dehydration temperatures of micas compared with hydroxides are in part a consequence of the shorter and stronger metal–hydroxide bonds in the micas.

Acknowledgments

We gratefully acknowledge the help and encouragement of Professors Clifford Frondel and Cornelius Hurlbut throughout our careers.

Most of the experiments were performed at the Massachusetts Institute of Technology in the Department of Earth and Planetary Sciences, and by means of the support of NSF grants GA-1109 and GA-13092 made to D. R. Wones. We appreciate the aid and support of J. V. Chernosky and R. W. Charles during the experimental work. G. E. Speicher of the Geophysical Laboratory performed the 10 kbar experiments in the laboratory of H. S. Yoder, Jr. G. V. Gibbs of Virginia Polytechnic Institute and State University and B. Mysen of the Geophysical Laboratory provided constructive reviews of the manuscript.

References

Appelo, C. A. J. (1978) Crystal energy and layer deformation of micas and related minerals. I. Structural models for 1M and $2M_1$ polymorphs. *Am. Mineral., 63,* 782–791.

Barnes, H. L. and W. G. Ernst (1963) Ideality and ionization in hydrothermal fluids: the system MgO–H_2O–NaOH. *Am. J. Sci., 261,* 129–150.

Bernal, J. D., D. R. Dasgupta and A. L. Mackay (1959) The oxides and hydroxides of iron and their structural inter-relationships. *Clay Mineral. Bull., 4,* 15–30.

Brown, G. E. (1970) *Crystal Chemistry of the Olivines.* Ph.D. Thesis, Virginia Polytechnic Institute and State University, Blacksburg, Virginia.

Burnham, C. W., J. R. Holloway and N. F. Davis (1969) Thermodynamic properties of water to 1000°C and 10,000 bars. *Geol. Soc. Am. Spec. Pap. 132.*

Donnay, G., J. D. H. Donnay and H. Takeda (1964a) Trioctahedral one-layer micas. II. Prediction of the structure from composition and cell dimensions. *Acta Crystallogr., 17,* 1374–1381.

———, N. Morimoto, H. Takeda and J. D. H. Donnay (1964b) Trioctahedral one-layer micas. I. Crystal structure of a synthetic iron mica. *Acta Crystallogr., 17,* 1369–1373.

Elleman, D. D. and D. Williams (1956) Proton positions in brucite crystals. *J. Chem. Phys., 25,* 742–744.

Eugster, H. P. and D. R. Wones (1962) Stability relations of the ferruginous biotite, annite. *J. Petrol., 3,* 82–125.

Foster, M. D. (1960) Interpretation of the composition of trioctahedral micas. *U. S. Geol. Surv. Prof. Pap., 354-B,* 11–46.

Frondel, C. and J. Ito (1966) Hendricksite, a new species of mica. *Am. Mineral., 51,* 1107-1123.

Garrels, R. M. and C. L. Christ (1965) *Solutions, Minerals, and Equilibria.* Harper and Row, New York.

Guidotti, C. V., J. T. Cheney and P. D. Conatore (1975) Interrelationship between Mg/Fe ratio and octahedral Al content in biotite. *Am. Mineral., 60,* 849–853.

Hazen, R. M. (1977) Temperature, pressure and composition: structurally analogous variables. *Phys. Chem. Minerals, 1,* 83–94.

——— and C. W. Burnham (1973) The crystal structures of one-layer phlogopite and annite. *Am. Mineral., 58,* 889–900.

——— and L. W. Finger (1977) Compression models for oxides and silicates (abstr.). *Geol. Soc. Am. Abstracts with Programs, 9,* 1008–1009.

——— and ——— (1978) The crystal structures and compressibilities of layer minerals at high pressure. II. Phlogopite and chlorite. *Am. Mineral., 63,* 293–296.

——— and C. T. Prewitt (1977) Effects of temperature and pressure on interatomic distances in oxygen-based minerals. *Am. Mineral., 62,* 309–315.

——— and D. R. Wones (1972) The effect of cation substitution on the physical properties of trioctahedral micas. *Am. Mineral., 57,* 103–129.

Hewitt, D. A. and D. R. Wones (1975) Physical properties of some synthetic Fe–Mg–Al trioctahedral micas. *Am. Mineral., 60,* 854–862.

Klingsberg, C. and R. Roy (1957) Synthesis, stability and polytypism of nickel and gallium phlogopite. *Am. Mineral., 42,* 629–634.

Lindqvist, B. (1966) Hydrothermal synthesis studies of potash-bearing sesquioxide–silica systems. *Geol. Fören. Stockholm Förh., 88,* 133–178.

MacDonald, G. J. F. (1955) Gibbs free energy of water at elevated temperatures and pressures with application to the brucite–periclase equilibrium. *J. Geol., 63,* 244–252.

McCauley, J. W. and R. E. Newnham (1971) Origin and prediction of ditrigonal distortions in micas. *Am. Mineral., 56,* 1626–1638.

———, ——— and G. V. Gibbs (1973) Crystal structure analysis of synthetic fluorophlogopite. *Am. Mineral., 58,* 249–254.

Pistorius, C. W. F. T. (1962) Thermal decomposition of the hydroxides of cobalt and nickel to 100 kilobars. *Z. Phys. Chem., 34,* 287–294.

Robie, R. A. and D. R. Waldbaum (1968) Thermodynamic properties of minerals and their related substances at 298.15°K (25.0°C) and one atmosphere (1.013 bars) pressure and at high temperatures. *U. S. Geol. Surv. Bull. 1251.*

Shannon, R. D. and C. T. Prewitt (1970) Revised values of effective ionic radii. *Acta Crystallogr., 26,* 1046–1048.

Slaughter, M. (1966) Chemical binding in silicate minerals. III. Application of energy calculations to the prediction of silicate mineral stability. *Geochim. Cosmochim. Acta, 30,* 323–339.

Takeda, H. and B. Morosin (1975) Comparison of observed and predicted structural parameters of mica at high temperature. *Acta Crystallogr., B31,* 2444–2452.

Wones, D. R. (1963) Phase equilibria of "ferriannite", K Fe_3^{+2} $Fe^{+3}Si_3O_{10}(OH)_2$. *Am. J. Sci., 261,* 581–596.

Yoder, H. S., Jr. and I. Kushiro (1969) Melting of a hydrous phase: phlogopite. *Am. J. Sci., 267-A,* 558–582.

Manuscript received, February 23, 1978; accepted for publication, April 7, 1978.